JOURNAL OF MATERIALS SCIENCE 22 (1987) 3939–3948

The effect of lattice defects induced by cathodic hydrogen charging on the apparent diffusivity of hydrogen in pure iron

JONG-LAM LEE*, JAI-YOUNG LEE
Department of Materials Science and Engineering, Korea Advanced Institute of Science and Technology, PO Box 131, Chongryang, Seoul, Korea

The variation of apparent hydrogen diffusivity with the applied current density and the types and amounts of hydrogen-induced damage caused by hydrogen during the cathodic charging of hydrogen in pure iron are investigated by thermal analysis techniques, and analysed in the light of theoretical models. Internal microcracks and microvoids are generated predominantly below 1 mA cm^{-2} and are the major trapping sites of hydrogen in pure iron when charging hydrogen cathodically. Blisters on the surface of iron specimens are found to be interconnected to the surface of the specimen through microcracks remaining in the vicinity of blisters. The peak temperature of hydrogen released from an internal microcrack or microvoid decreased as the applied current density is increased. The apparent diffusivity of hydrogen at 458 K decreases linearly with the reciprocal value of the square root of applied current density during cathodic charging. This implies that the amounts of internal microcracks or microvoids are linearly proportional to the lattice hydrogen solubility or the square root of the applied current density.

1. Introduction

It is known that the presence of internal hydrogen in a wide variety of metals and alloys gives rise to the generation and growth of planar cracks along both grain boundaries and crystallographic lattice plans [1–5]. The precise method of crack nucleation during hydrogen charging has been accepted as relating to a localized concentration of hydrogen at suitable heterogeneities such as grain boundaries [3], second-phase particles [2] and tangled dislocations [6]. The presence of such cracks is more dangerous as it leads to the leakage of gas or liquid.

Hydrogen-induced defects such as internal microvoids or microcracks and dislocations are formed by the precipitation of hydrogen molecules at some sites [7, 8], when the alloys are charged with high-fugacity hydrogen evolved cathodically in acid solutions containing promoting species such as As_2O_3 and AsH_3 [9, 10]. Therefore a study of the damage caused by hydrogen is important for interpreting the role of hydrogen in the embrittlement of steels, because it may act as variables of hydrogen embrittlement such as composition, microstructure, process history, strength level, etc., and it also makes the permeability of hydrogen low [11–16]. Several researchers [9, 10, 16] have claimed that hydrogen-induced defects could be nucleated during the electro-permeation of iron or steel, as indicated by maxima in the relation of the rate of permeation with time. The values of the critical current density for the generation of such maxima were 0.8 to 4.3, 13.5 and 100 mA cm^{-2} for Armco iron [9], AISI 1090 steel [10] and quenched and tempered AISI 4340 steel [17], respectively. However, Poperlings and Schwenk [18] concluded that the maximum in the plot of permeability against time is not due to defect generation during cathodic charging but to the decreased effectiveness of promoters such as As_2O_3 and $HgCl_2$ with permeation time. Although a large volume of work on the production of hydrogen-induced damages during cathodic charging has been carried out as above, the fundamental aspects of the process have not been understood clearly. In particular, hydrogen-induced damage has not been investigated in the light of trapping sites of hydrogen, and its effect on the diffusion of hydrogen in iron has not been established clearly because of experimental difficulties, as it is continuously generated during the electro-permeation experiment. In general, hydrogen trapping in steel has been mainly studied by using the hydrogen permeation method [19, 20]. The weak point of this method is not observing the hydrogen escaped from the defects directly. This is solved by developing the thermal analysis technique [21].

This work therefore stresses the determination of the types and the amounts of lattice defect and the detection of a major site of hydrogen among such defects, created during the cathodic hydrogen charging of pure iron, by the thermal analysis technique. Thermal analysis data were utilized in the investigation of the variation of apparent hydrogen diffusivity with the amount of lattice defects, through the mathematical model suggested in this work. The

Present address: Electronics and Telecommunications Research Institute, PO Box 8, Daedog Danju, Daejeon, Choongnam, Korea.

0022–2461/87 $03.00 + .12

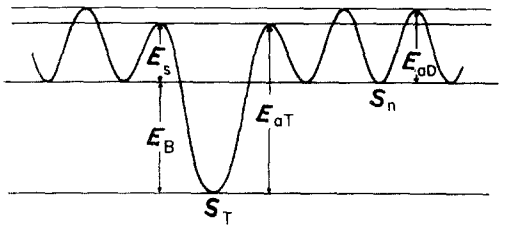

Figure 1 The energy level of hydrogen around the trap site.
E_{aD}: diffusion activation energy of hydrogen in normal lattice
E_S: saddle point energy
E_{aT}: trap activation energy
E_B: trap binding energy
S_n: normal lattice site
S_T: trapping site.

characteristics of hydrogen evolution from microvoids are examined by carrying out the thermal analysis immediately after the cathodic charging of pure iron.

2. Theory of thermal analysis

Under the assumption that the escaping reaction of hydrogen from the trap site in Fig. 1 is a thermally activated process, the hydrogen evolution rate from a trapping site can be written as

$$\frac{dX_T}{dt} = A_c (1 - X_T) \exp\left(-\frac{E_{aT}}{RT}\right) \quad (1)$$

where X_T is a fractional amount of hydrogen evolved from a trapping site at time $t \neq 0$, T is the absolute temperature, R is the gas constant and A_c a constant. The detailed physical meaning of Equation 1 has been discussed in other articles [21–24].

3. Experimental procedure

Electrolytic iron was melted in an induction furnace, and this ingot was remelted in a vacuum arc remelting furnace to remove gas elements. After forging at 1423 K the ingot was normalized for two hours at 1173 K. This ingot was cut into a rectangular shape with a thickness of 0.1 cm. The chemical composition of the pure iron used in this experiment is given in Table I.

In order to charge the hydrogen cathodically, a pure iron specimen with a rectangular shape (1 mm × 6 mm × 14 mm) was polished chemically after surface grinding with emery paper No. 1200. Cathodic charging was performed at room temperature in a 10% sulphuric acid solution with a recombination poison agent of 10 mg As_2O_3 per litre. In the case of cathodic charging, a constant time of 12 h was employed to ensure a uniform distribution of hydrogen throughout the specimen. The applied current density was varied from 0.5 mA cm^{-2} to higher values. For cathodic charging at a constant current density of 10 mA cm^{-2}, the charging time was varied from 1.0 to 12.0 h. No external stress was applied during cathodic charging.

TABLE I Chemical composition of specimen (wt p.p.m.)

C	N	S	P	Ni	Cr	Si	Mn
–	35	40	–	511	–	–	–

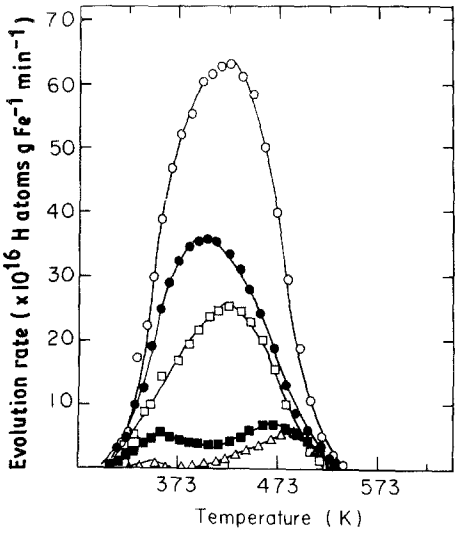

Figure 2 Thermal analysis results performed after cathodic charging for 12 h at various current densities (first thermal analysis): (△) 0.5, (■) 1, (□) 5, (●) 10, (○) 20 mA cm^{-2}.

A cathodically charged specimen was held under an argon atmosphere at room temperature for 2.0 h in the thermal analysis reactor and then heated at a uniform rate of 3 K min^{-1}, and the amount of hydrogen escaping from the specimen was analysed quantitatively by gas chromatography to obtain the evolution rate (first thermal analysis). To reduce the possibility of the annihilation of dislocation during heating, thermal analysis experiments were carried out up to 623 K. It was carefully arranged that the hydrogen dissolved in the iron specimen by cathodic charging escaped completely from the specimen in the first thermal analysis. The details of the thermal analysis method have been presented in previous papers [23, 25, 26].

To determine the types and amount of damage caused by hydrogen during cathodic charging, the following experiment was carried out. After the first thermal analysis the specimen was repolished chemically, and then charged with hydrogen for 16 h at 458 K under atmospheric hydrogen pressure to prevent the annihilation of dislocations during the gaseous charging of hydrogen, which may be nucleated during cathodic charging, and then quenched into ice-water under a hydrogen atmosphere. The subsequent procedures of the second thermal analysis were the same as those of the first thermal analysis. The details of the gaseous charging method were presented in a previous paper [23]. The heights and the temperatures of the thermal analysis peaks during the first and second thermal analysis are reproducible under the same hydrogen charging conditions.

4. Experimental results

Two evolution rate peaks of hydrogen appear in the thermal analysis performed after cathodic charging for 12 h at each current density, as shown in Fig. 2. At a current density of 1 mA cm^{-2}, peaks for hydrogen released from the iron specimen appear at 339 and 485 K. The heights increase with increasing applied current density. The second evolution rate peak appearing at 485 K shifts toward lower temperature with an increase of the applied current density, but the

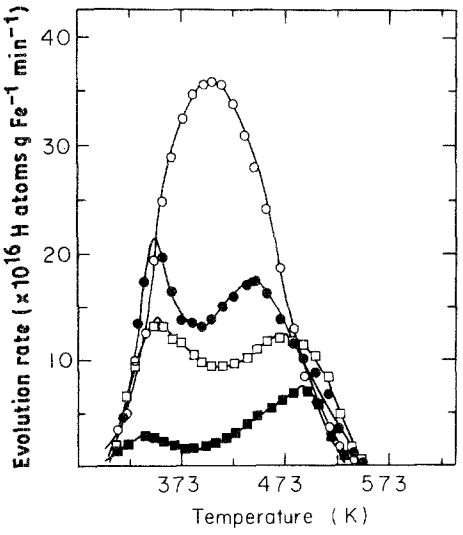

Figure 3 Thermal analysis results obtained after cathodic charging for various times at a constant current density of 10 mA cm^{-2} (first thermal analysis): (■) 1, (□) 2, (●) 3, (○) 12 h.

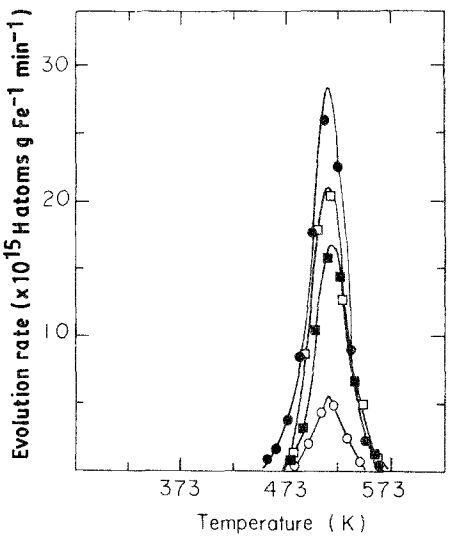

Figure 5 Results of second thermal analysis of specimens charged cathodically with hydrogen for various times at a constant current density of 10 mA cm^{-2}: (○) 0 (as-received), (■) 1, (□) 2, (●) 12 h.

temperature of the first peak at 339 K is independent of the magnitude of the current density. When the hydrogen charging time is changed at a constant current density of 10 mA cm^{-2}, the tendencies of a change of peak temperature for the second peak at 485 K and an increase of the heights of both peaks, with an increase of charging time, are similar to the results in Fig. 2, as shown in Fig. 3. On increasing the hydrogen charging time the heights of both peaks increase and the second peak at 485 K is shifted toward the lower temperature region.

Fig. 4 contains the results of the second thermal analysis performed to decide more clearly the types and the amounts of hydrogen-induced defects generated by cathodic charging. Only one evolution rate peak for hydrogen appears as 518 K, and the height of the peak (which means the amount of hydrogen released from the lattice defect created during cathodic changing) increases with applied current density.

Fig. 5 shows that the longer is the hydrogen charging time at a constant applied current density of 10 mA cm^{-2}, the higher is the height of the evolution rate peak at 518 K. This indicates that one type of lattice defect in the case of the iron specimen is mainly generated during cathodic charging. The height of the peak at 518 K will be diminished to the level of the as-received specimen (non-cathodically charged specimen) because cold-worked iron is completely recrystallized in the vicinity of 873 K [19], if it is related to dislocations. If it is related to microvoids, the height of the peak at 518 K will not be changed. When the second thermal analysis of an annealed specimen was performed, the height of peak at 518 K was nearly the same as that of a non-annealed specimen as shown in Fig. 6. This result supports the idea that the evolution rate peak appearing at 518 K in the second thermal analysis corresponds to the hydrogen released from internal microcracks or microvoids generated during cathodic charging.

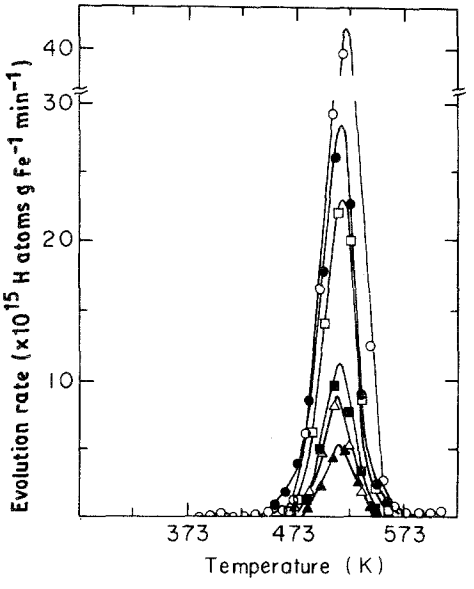

Figure 4 Results of second thermal analysis of specimens charged cathodically with hydrogen for 12 h at various current densities: (▲) 0 (as-received), (△) 0.5, (■) 1, (□) 5, (●) 10, (○) 20 mA cm^{-2}.

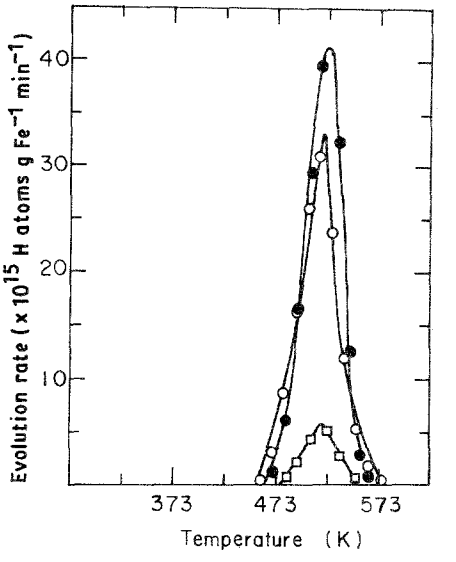

Figure 6 Variation of peak height of specimen charged cathodically with hydrogen for 12 h at a current desity of 20 mA cm^{-2} (second thermal analysis): (□) as-received, (●) before annealing, (○) after annealing.

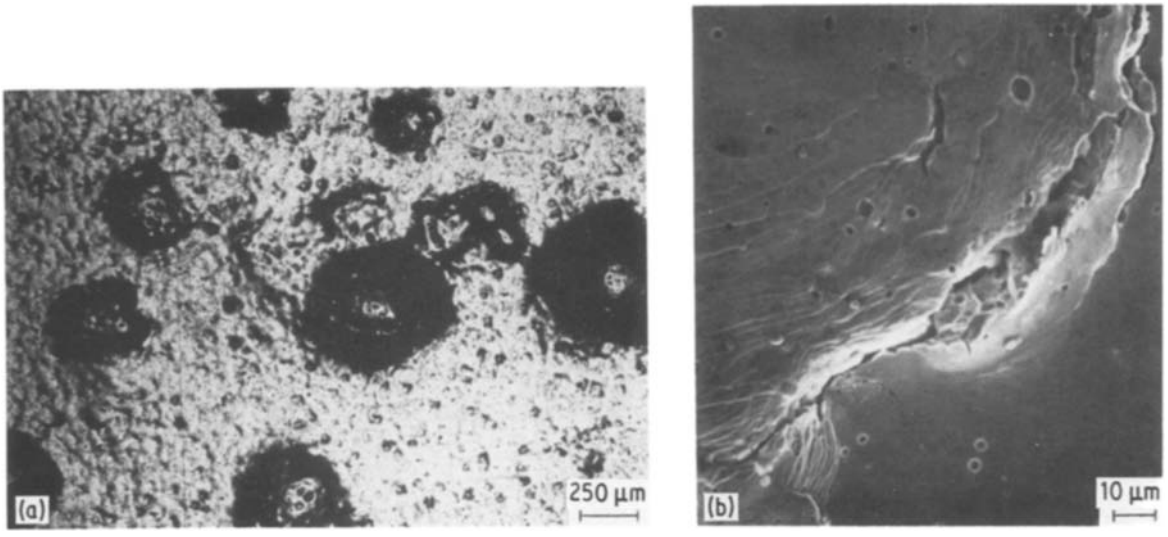

Figure 7 (a, b) Surface blisters generated during cathodic charging.

To confirm the generation of internal microvoids or microcracks during cathodic charging, the microstructure of iron cathodically charged for 12 h at a current density of 10 mA cm^{-2} is shown in Fig. 7a. Careful examination of the surrounding area of a blister by a scanning electron microscope (SEM) intimates that many microcracks surrounding it play the role of interconnecting the surface of the specimen and the inside of the blister. A mark of plastic deformation with a ripple shape directing the production of a dislocation is also found in Fig. 7b. The observations of microstructure include the fact that blisters formed on the surface of the specimen during cathodic charging are interconnected to the specimen surface through microcracks.

Observing the cross-section of a specimen under an optical microscope, a large number of internal microvoids or microcracks isolated from the free surface are produced by cathodic charging as shown in Fig. 8, which is consistent with reports by others [3, 4].

For the purpose of establishing the nucleation of hydrogen-induced microvoids during cathodic charging, iron cathodically charged for 12 h at 10 mA cm^{-2} was fractured in a liquid nitrogen bath. Fracture proceeded mainly through the grain-boundary as shown in Fig. 9a. Investigating the grain-boundary facet, a lot of microvoids which were never detected in hydrogen-free specimens are observed as in Fig. 9b. Comparing this fractograph with the second thermal analysis results in Figs 4, 5 and 6, it is clear that internal microvoids or microcracks which act as trapping sites of hydrogen are generated during cathodic charging. Observation under a transmission electron microscope (TEM) [6] after cathodic charging of an iron specimen at 10 mA cm^{-2} supports the nucleation of internal microvoids or microcracks due to the precipitation of hydrogen molecules. Takeyama and Takahashi [6] also found that a multiplication of dislocations occurred around a nucleated microvoid, owing to plastic deformation by the accumulation of hydrogen molecules.

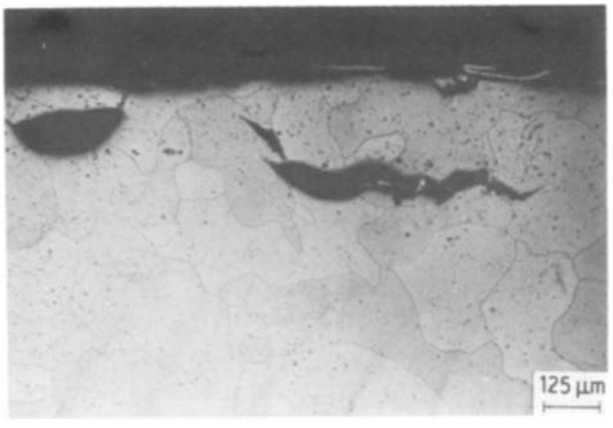

Figure 8 Internal microcracks after cathodic charging.

In Fig. 8, plastic deformation directing the production of dislocations is found, and Takeyama and Takahashi [6] found hydrogen-induced dislocation under TEM. However, the evolution rate peak of hydrogen released from dislocations did not appear in the second thermal analysis experiment. A possible reason for this is that when the total amount of hydrogen trapped in dislocations is slight, as it is when the increase of dislocation density is induced by cathodic charging, it is smaller than the sensitivity of gas chromatography (10^{14} hydrogen atoms per gram of iron per minute). This is also established by the microstructural results, in which recrystallization or a grain-size variation are not detected when the annealing of cathodically charged iron for 12 h at 20 mA cm^{-2} is executed above the temperature of recrystallization.

The evolution rate peak of hydrogen representing internal microvoids or microcracks diminished a little after annealing as shown in Fig. 6, and this result is supported by the previous results for AISI 4340 steel [22] that the hydrogen evolution peak representing microvoids for the 45% cold-worked specimen diminishes with repetition of the thermal analysis, and by the results of Evans and Rollason [28] in which they suggested that the large number of microvoids nucleated by cold-working decreased with increasing annealing temperature.

5. Discussion

5.1. First thermal analysis

In previous work [25, 29], evolution rate peaks of hydrogen were observed at 368, 453 and 513 K at the

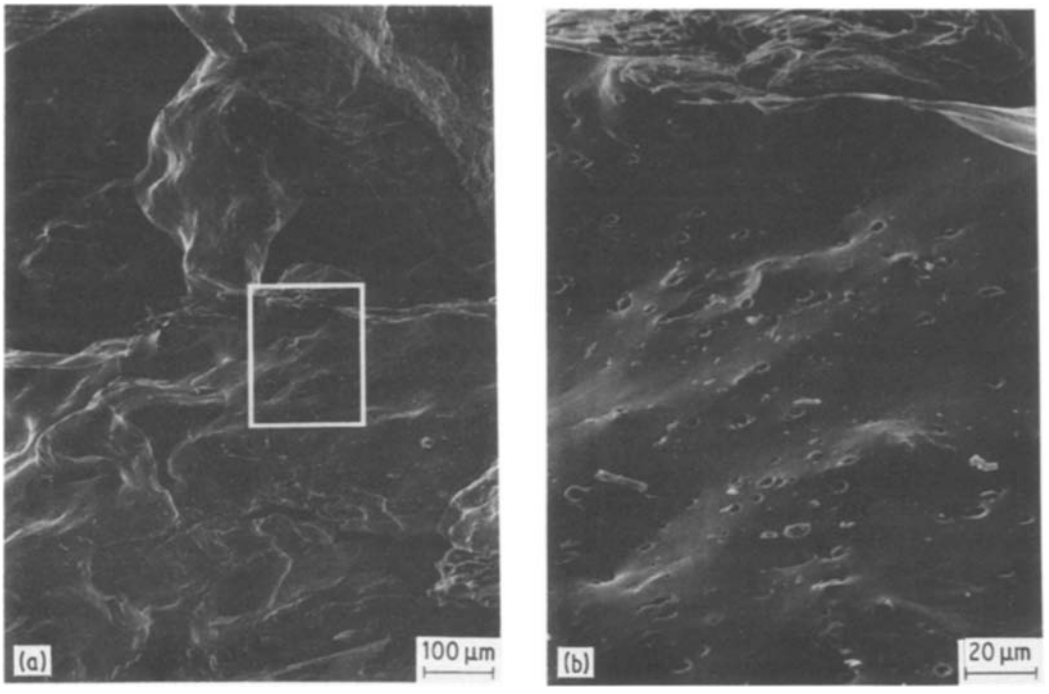

Figure 9 A cross-section by SEM of a sample fractured in a liquid nitrogen bath after cathodic charging: (a) low magnification, (b) high magnification.

same heating rate as this work, $3\,K\,min^{-1}$, when gaseous hydrogen was charged thermally into pure iron with a cylindrical shape of 5 mm diameter. Analysis has suggested that the peak at 368 K corresponds to hydrogen release from normal lattice sites, maintaining a dynamic local equilibrium with that from grain boundaries; the peak at 453 K corresponds to dislocations and the peak at 513 K to microvoids. The 363 K peak, relating to a reversible trap site such as a grain boundary, shifts toward the lower temperature region as the thickness of specimen is reduced. On the other hand, the peak temperature of hydrogen escaping from microvoids, which act as an irreversible trap for hydrogen diffusion at room temperature, is independent of the thickness of the specimen. Therefore it is believed that the 339 K peak in Figs 2 and 3 is related to hydrogen evolution from normal lattice sites, maintaining a dynamic local equilibrium with that from grain boundaries, considering that the thickness of iron (1 mm) is thinner than that in previous work [25]. The 485 K peak in the case of cathodic charging at $1\,mA\,cm^{-2}$ might be due to hydrogen released from internal microvoids or microcracks; this is supported by the results of the second thermal analysis shown in Figs 4, 5 and 6. However, the peak for internal microvoids or microcracks in the first thermal analysis, after cathodic charging at $1\,mA\,cm^{-2}$, shows up at a temperature which is lower by about 30 K than that in the second thermal analysis (see Fig. 2). This peak is shifted toward the lower temperature region with increases of applied current density and hydrogen charging time.

In order to analyse the migration of the evolution rate peak at 485 K in the first thermal analysis, the following analysis is possible. The hydrogen pressure in an internal microcrack or microvoid becomes high with increases of the applied current density and hydrogen charging time. Considering an increment of lattice hydrogen solubility with the input fugacity of hydrogen [27, 32] and the concentration profile of hydrogen with the charging time (see Fig. 10). Therefore there is a possibility that the hydrogen pressure in an internal microvoid or microcrack affects the variation of temperature of the evolution rate peak of hydrogen released from internal microvoids or microcracks. Recently Bozso *et al.* [30] found that the desorption rate of hydrogen atoms from an iron surface obeys second-order reaction kinetics, and the activation energy of desorption of hydrogen was determined to be $26 \pm 1\,kcal\,mol^{-1}$. It is known that the heat of solution of hydrogen in iron is about 6.0 to $7.0\,kcal\,mol^{-1}$ [25, 31]. Therefore under the assumption that the hydrogen molecules in an internal microvoid or microcrack, precipitated during cathodic charging, are adsorped into the normal lattice site of the iron matrix, the rate of dislocation of hydrogen from the internal microvoid or microcrack may be written as

$$N(t) = -\frac{dP}{dt} = v_n P^n \exp(-Q/RT) \quad (2)$$

where n is the order of the desorption reaction, P is the pressure of hydrogen, v_n is the rate constant and Q is the activation energy of dissolution.

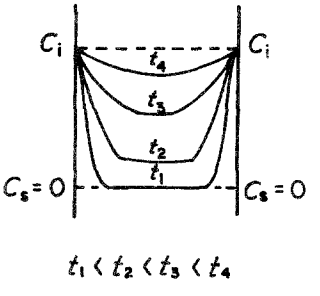

Figure 10 Variation of hydrogen concentration with charging time.

We will first consider a linear change of sample temperature with time ($T = T_0 + \phi t$) and assume that Q is independent of P. Equation 2 is solved to find the temperature (T_c) at which the dissolution rate is a maximum; then

$$Q/RT_c^2 = (v_1/\phi) \exp(-Q/RT_c) \quad \text{for } n = 1 \quad (3a)$$

$$= (2P_c v_2/\phi) \exp(-Q/RT_c) \quad \text{for } n = 2 \quad (3b)$$

where P_c is the hydrogen pressure at $T = T_c$.

In the thermal desorption theory for hydrogen gas [30], the initial surface coverage (σ_0) has a linear relationship with the coverage (σ_p) at $T = T_c$, such as $\sigma_0/\sigma_p \approx 2$. Therefore it is reasonable to assume the relationship

$$P_0 = aP_c \quad (4)$$

where a is a constant and P_0 is the initial hydrogen pressure in an internal microvoid. Substituting Equation 4 into Equation 3b and taking the logarithm of both sides,

$$\ln\left(\frac{\phi}{T_c^2 P_0}\right) = \ln\left(\frac{2Rv_2}{Qa}\right) - \frac{Q}{RT_c} \quad (5)$$

Bozso *et al.* [30] obtained a series of thermal desorption spectra recorded with a heating rate of 7 K sec^{-1} from Fe(1 1 0) after H_2 exposures between 0.4 and 3500 L at 140 K, and found that the hydrogen desorption peak shifts towards lower temperatures with increasing coverage, indicating second-order kinetics. In this work, the temperature at which maximum hydrogen evolution from the internal microvoid or microcrack occurred was shifted towards lower temperatures with increasing applied current density and hydrogen charging time. This means that the hydrogen evolution reaction from an internal microvoid or microcrack obeys second-order reaction kinetics. Thus the order of the dissolution reaction can be determined from the behaviour of the maximum in the hydrogen evolution rate curve with hydrogen pressure. Returning to the second-order case, it can be seen from Equation 3b that T_c now depends on the hydrogen pressure. The activation energy for this dissolution of hydrogen may be found from the slope in a plot of $\ln(\phi/T_c^2 P_0)$ against $1/T_c$.

The experimental results in Fig. 11 support second-order reaction kinetics in evolution of hydrogen from internal microvoids or microcracks. When iron cathodically charged for 12 h at 10 mA cm^{-2} is degassed for 72 h at room temperature in a vacuum chamber, the hydrogen evolution rate peak for internal microvoids or microcracks shifts towards higher temperatures, in comparison with the non-degassed iron. This must be due to the decrease of hydrogen pressure by hydrogen release from internal microvoids or microcracks during the degassing treatment of cathodically charged iron. This is, Fig. 11 confirms the second-order reaction kinetics of hydrogen evolution from internal microvoids. The peak for hydrogen released from normal lattice sites, maintaining dynamic local equilibrium with that from grain boundaries, disappears as a result of vacuum degassing for 72 h at room temperature.

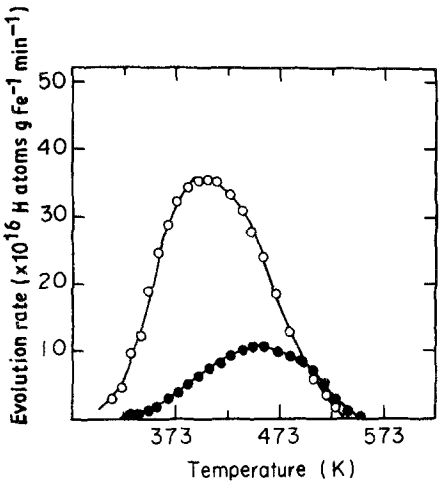

Figure 11 (●) Iron degassed in a vacuum for 72 h at room temperature after cathodic charging for 12 h at 10 mA cm^{-2}; (○) iron held in a vacuum for 2 h.

In cathodic charging for a high applied current density (above 5 mA cm^{-2}) and long hydrogen charging time (above 12 h), the evolution rate peak for hydrogen released from normal lattice sites, maintaining dynamic local equilibrium with that from grain boundaries, could not be detected in thermal analysis spectra (see Figs 2 and 3). This might be due to the duplication of lattice peak and microvoid peak because the microvoid peak shifts towards lower temperatures with increasing applied current density and hydrogen charging time.

5.2. Second thermal analysis

It is established in this work that internal microcracks or microvoids acting as trapping sites for hydrogen are created more dominantly than dislocations, and the amounts increase with the applied current density. Internal microcracks or microvoids begin to originate above an applied current density of 1.0 mA cm^{-2} during cathodic charging. This is closely comparable with the theoretical result suggested by Lee and Lee [32], in which it is calculated that the critical current density for the generation of permanent hydrogen-induced damage during cathodic charging in the solution used in this work is about 0.5 to 1.0 mA cm^{-2}. The experimental results are in the range of those of Beck *et al.* [9], 0.8 to 4.3 mA cm^{-2}. Thus internal microvoids or microcracks are the major trapping sites of hydrogen in pure iron, if the hydrogen is charged cathodically. Up to now, there remained the issue of "how the internal microcracks or microvoids during cathodic charging effect the apparent hydrogen diffusivity?" because the permeability of hydrogen increases again steadily after the formation of maxima in the relation of the rate of permeation to time in the permeation experiments [9, 10, 17]. This problem can be solved by using the following model if the amounts of hydrogen trapped in each trapping site can be determined quantitatively, which is possible by the thermal analysis method.

5.2.1. The effect of hydrogen-induced microvoids or microcracks on the apparent hydrogen diffusivity

McNabb and Foster [33] have derived Equation 6 below, a relation between the lattice hydrogen diffusivity (D_L), the apparent hydrogen diffusivity (D_A) and the trap parameters (α, β) by considering the trapping rate and detrapping rates from a trapping site:

$$\frac{a^2}{6D_A} = \frac{a^2}{D_L}\left[\frac{1}{6} + \frac{\alpha}{2\beta} + \frac{\alpha}{\beta^2} - \frac{\alpha}{\beta^3}(1+\beta)\log(1+\beta)\right] \quad (6)$$

where $\alpha = N_T k/p$, $\beta = C_L k/p$, k is the transition probability for hydrogen transport from a lattice site to a trapping site and p is the transition probability for hydrogen transport from a trapping site to a lattice site. α and β are dependent upon the magnitude of the trap density (N_T) and lattice solubility of hydrogen (C_L), respectively.

It has been established that the trap activation energy for hydrogen release from a microvoid is 40.31 kJ mol^{-1} [25] and the activation energy for hydrogen diffusion through the normal lattice is 6.91 kJ mol^{-1} [31]. If the saddle-point energy for a microvoid is equal to 6.91 kJ mol^{-1}, the trap binding energy of hydrogen for the microvoid is 33.4 kJ mol^{-1}. A previously published paper [32] states that the trap density for the site existing originally in an iron specimen is about 4×10^{18} sites per gram of iron, which is consistent with the results of Oriani [34]. The trapping parameters and trap occupancy fraction n, computed by using Equations 6 and 10 (below) under the assumption that $dn/dt = 0$, for a microvoid with a binding energy of 33.4 kJ mol^{-1} and a trap density of 4×10^{18} sites per gram of iron, are 0.771 and 3.851×10^{-3}, respectively, when the gaseous hydrogen is charged into pure iron at 458 K. The lattice solubility of hydrogen in pure iron is derived by Equation 18 of Kuichi and McLellan [31]; the calculated ratio of α to β is about 2.002×10^2 at a temperature of 458 K under atmospheric hydrogen pressure. So one can make the assumptions that the trap site is occupied only sparsely by hydrogen (β, $n \ll 1$) and is much higher than ($\alpha \gg \beta$) at the charging temperature, 458 K. In other words, microvoids play the role of reversible traps for hydrogen at 458 K, which can be also presumed qualitatively from the fact that the maximum evolution rate of hydrogen from microvoids occurred at 518 K, which is similar to the hydrogen charging temperature. At room temperature the microvoids will, however, be saturated with hydrogen, and surely act as irreversible traps as discussed by Pressouyre and Bernstein [27]. Therefore Equation 6 is simplified to

$$D_L = D_A(1 + \alpha) \quad (7)$$

The energy level of hydrogen around the trapping site is assumed to be as in Fig. 1, and k and p can be written as

$$k = v_0 \exp(-E_s/RT)$$
$$p = v_1 N_L \exp[-(E_s + E_B)/RT] \quad (8)$$

v_0 and v_1 are the vibrational frequencies of hydrogen atoms at normal lattice sites and trapping sites, respectively. If it can be assumed that both vibration frequencies (v_0, v_1) are the same, then Equation 8 can be expressed as

$$\alpha = \frac{N_T}{N_L}\exp\left(\frac{E_B}{RT}\right) \quad (9)$$

Combining Equations 7 and 9,

$$D_L = D_A\left[1 + \frac{N_T}{N_L}\exp\left(\frac{E_B}{RT}\right)\right] \quad (10)$$

where N_L is the number of interstitial sites in the normal lattice.

The variation of the hydrogen occupancy fraction of the trap site with time (dn/dt) is expressed [33] as

$$\frac{dn}{dt} = kC_L(1 - n) - pn \quad (11)$$

If equilibrium is established between hydrogen in trapping sites and in interstitial sites of the normal lattice, the rate of change of the trap occupancy fraction with time is constant ($dn/dt = 0$). In the case of microvoids the trap occupancy fraction at the hydrogen charging temperature is generally very small ($n = 3.646 \times 10^{-3}$) or $(1 - n) \approx 1$. Then

$$\frac{C_T}{C_L} = \frac{N_T}{N_L}\exp\left(\frac{E_B}{RT_H}\right) \quad (12)$$

where C_T is the number of hydrogen atoms trapped in trapping sites per gram of iron and T_H is the hydrogen charging temperature.

Comparing Equation 10 with Equation 12, we may derive the equation

$$\frac{D_L}{D_A} = 1 + \frac{C_T}{C_L} \quad (13)$$

In this work, an attempt is made to determine the variation of the apparent diffusivity of hydrogen in specimens which were charged with hydrogen electrolytically under various conditions, relative to that of a non-charged specimen. Letting the apparent hydrogen diffusivity of a reference specimen be D_{AR} and the apparent diffusivity of a specimen with a variable amount of trapping sites be D_{AV}, the ratio of apparent hydrogen diffusivities of both specimens is

$$\frac{D_{AV}}{D_{AR}} = \frac{C_L + C_{TR}}{C_L + C_{TV}} \quad (14)$$

where C_{TR} and C_{LR} are the number of hydrogen atoms trapped in trapping sites per gram of iron for a reference specimen, and a specimen with a variable amount of trapping sites respectively, one can determine the ratio of apparent hydrogen diffusivities readily from Equation 14, if the amount of hydrogen trapped in hydrogen-induced microvoids or microcracks can be measured quantitatively.

Recently the authors [25, 29] have suggested a hydrogen retrapping theory. During rapid cooling of metal with a b c c structure to room temperature, after charging the specimen under atmospheric hydrogen pressure at a high temperature (i.e. thermal charging),

the supersaturated hydrogen in interstitial sites of a normal lattice at the quenching temperature is retrapped into trapping sites which are not occupied with hydrogen at the charging temperature. In other words, a new equilibrium state between the supersaturated hydrogen and trapping sites results. Therefore the total amount of hydrogen trapped in one type of trapping site is equivalent to the sum of hydrogen trapped at the charging temperature and hydrogen retrapped at lower temperatures. In thermal analysis of the hydrogen-charged specimen, the amount of hydrogen released from one type of trapping site is represented by

$$C_{T_{TA.R.V}} = C_{T_{R.V}} + g(C_{LH} - C_{LR}) = \left[N_T \frac{C_0}{N_L} \exp\left(\frac{E_B - E_0}{RT_H}\right)\right] \Big/ \left[1 + \frac{C_0}{N_L} \exp\left(\frac{E_B - E_0}{RT_H}\right)\right] + g(C_{LH} - C_{LR}) \quad (15)$$

where R and V mean the specimen state before and after cathodic charging, respectively, g is the retrapping factor of hydrogen, and C_{LH} and C_{LR} are the lattice hydrogen solubilities at charging temperatures T_H and T_R (the quenching temperature), respectively. The trapping factor g for a given trap is the fraction of hydrogen retrapped into non-occupied trapping sites. In other words, $g = 1$ means that all excess hydrogen formed by quenching at room temperature is retrapped completely into the non-occupied trapping sites, whereas at $g = 0$, hydrogen is not retrapped by evolution from the specimen.

Considering a charging temperature of 458 K, C_{LH} is much larger than C_{LR}. Therefore Equation 15 can be rewritten as

$$C_{T_{TA.R.V}} = C_{T_{R.V}} + gC_{LH} \quad (16)$$

Substituting Equation 16 into Equation 14, we derive the equation

$$\frac{D_{AV}}{D_{AR}} = \frac{C_{T_{TA.R}} + C_L(g - 1)}{C_{T_{TA.V}} + C_L(g - 1)} \quad (17)$$

Therefore (D_{AV}/D_{AR}) at the hydrogen charging temperature can be determined from Equation 17 because the amount of trapped hydrogen in the reference specimen ($C_{T_{TA.R}}$) and the variable specimen ($C_{T_{TA.V}}$) can be determined from the areas of the evolution rate peaks of hydrogen evolved with hydrogen-induced damage for each specimen in the thermal analysis technique.

To examine the variation of the ratio of apparent hydrogen diffusivities (D_{AV}/D_{AR}) using Equation 17, we need to know the lattice solubility of hydrogen in pure iron. In this work, the equation derived by McLellan [29] is used:

$$C_L = 3.7P^{1/2} \exp\left[-27.3 \pm 1.4(\text{kJ mol}^{-1})/RT\right] \times \frac{[\text{cm H}_2(\text{NTP})]}{[\text{cm}^3\,\text{Fe}]} \quad (18)$$

(D_{AV}/D_{AR}) at 458 K determined from a combination

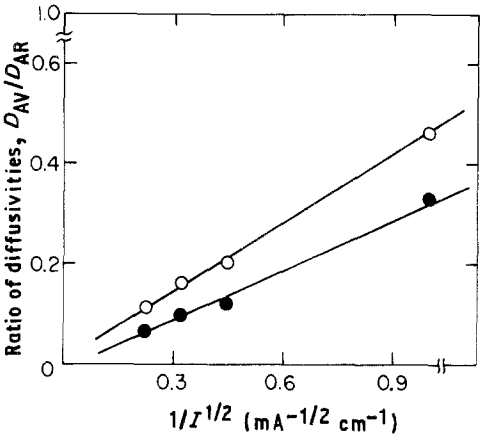

Figure 12 The ratio of apparent hydrogen diffusivities (D_{AV}/D_{AR}) at 458 K against the reciprocal value of the square root of applied current density; charging time 12 h (second thermal analysis). (○) $g = 0$, (●) $g = 1$.

of the results of the second thermal analysis (Fig. 4) and Equation 17 decreases linearly with a decrease of the reciprocal value of the square root of applied current density as shown in Fig. 12; A D_{AV} is reduced as the applied current density increases. For example, in the case of iron cathodically charged for 12 h at an applied current density of 10 mA cm^{-2}, D_{AV} at 458 K is reduced by about one order of magnitude compared with the reference specimen (non-cathodically charged iron). The relationship between (D_{AV}/D_{AR}) and N_T can be represented by combining Equations 12 and 17 to give

$$\frac{D_{AV}}{D_{AR}} = \frac{N_L(2g - 1) + N_{TR} \exp(E_B/RT_H)}{N_L(2g - 1) + N_{TV} \exp(E_B/RT_H)} \quad (19)$$

The physical meaning of Equation 19 is that the ratio decreases linearly with the reciprocal of N_{TV} because several factors such as N_L, g, E_B, T_H and N_{TR} have constant values.

Comparing Equation 19 with Fig. 12, the trap density (N_{TV}), implying the permanent damage induced by hydrogen during cathodic charging, increases linearly with the square root of applied current density. The relationship between the height of the peak representing the internal microvoids or microcracks (contained in Fig. 4) and the square root of the applied current density is given in Fig. 13, which shows that the relationship is linear. This suggests that the amount of internal microvoids or microcracks is linearly dependent upon the square root of the applied current density, because the trap occupancy fraction n for one type of trapping site is constant at a constant charging temperature. It has been shown extensively that a linear relationship holds between the lattice hydrogen solubility and the square root of the applied current density during cathodic charging and/or electro-permeation experiments [27, 32]. In view of the appearance of hydrogen-induced damage in this connection, the amount of internal microcracks or microvoids increases linearly with the amount of hydrogen dissolved into interstitial sites of the normal lattice of pure iron during cathodic charging of hydrogen. Fig. 14 shows that the area fraction of surface blisters observed on the iron surface by optical microscopy is

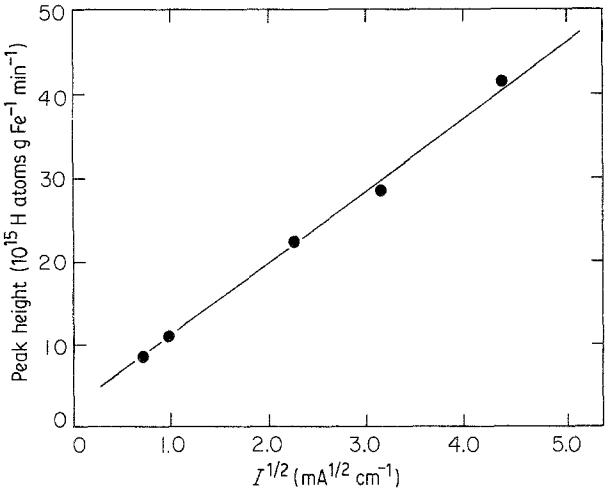

Figure 13 Relationship between the microvoid peak height in Fig. 4 and the square root of applied current density.

a linear function of the square root of applied current density. This supports the above suggestion which is consistent with the previous result [32].

In a previous paper [21], evolution rate peaks of hydrogen escaping from grain boundaries were observed. However, they were not observed in this case. This is due to the difference in the hydrogen charging temperature, i.e. 673 K in the experiments of Choo and Lee [21] and 458 K in this work. Modifying Equation 12, C_T is given as

$$C_T = \frac{N_T}{N_L} C_0 \exp\left(\frac{E_B - E_0}{RT_H}\right) \quad (20)$$

In Equation 20, the amount of hydrogen trapped in grain boundaries (C_T) decreases as the hydrogen charging temperature (T_H) decreases, because the trap binding energy (E_B) is lower than the heat of solution of hydrogen. Therefore, the reason why a peak for hydrogen released from grain boundaries does not appear is that a relatively small amount of hydrogen is trapped in grain boundaries owing to the low temperature of hydrogen charging.

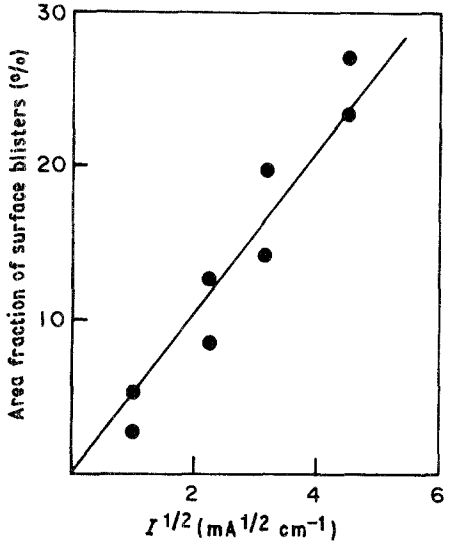

Figure 14 Area fraction of surface blisters against the square root of the applied current density; charging time 12 h (second thermal analysis).

Recently, Lee and Lee [32] have calculated the trap occupancy fraction of hydrogen ($n = C_T/N_T$) as 0.37, by using their own theoretical model for the generation of hydrogen-induced defects when the cathodic charging of pure iron is carried at 1.0 mA cm^{-2} in the same solution as in this work. This implies that hydrogen-induced internal microvoids and/or microcracks are nucleated predominantly at special sites such as the triple points of grain boundaries [4] and the tangles of dislocations produced by the precipitation of hydrogen molecules during cathodic charging. This supports the concept of a critical concentration of hydrogen for the generation of internal microvoids and/or microcracks [11–13]. It follows that during cathodic charging for a constant time, hydrogen atoms are trapped predominantly at the special trapping sites and not at other traps such as grain boundaries or dislocations. At a particular concentration of hydrogen at special trapping sites, internal microcracks start to form. It may be seen from the micrographs in Fig. 9 that internal microcracks traverse the grain boundary. The special trapping site is believed to be a triple point of grain boundaries.

At these positions the critical concentration of hydrogen is related to the input fugacity of hydrogen or the input current density during cathodic charging. Accordingly, it is believed that the critical concentration of hydrogen for the generation of internal microvoids and/or microcracks corresponds to an input current density of 1.0 mA cm^{-2}, when pure iron is cathodically charged with hydrogen in a 10% sulphuric acid solution where a recombination poison of about 10 mg l^{-1} As_2O_3 is added. However, the critical current density for the generation of hydrogen-induced defects during cathodic charging should be dependent upon the type of electrolytic solution and the amount of recombination poison, because the absorbed amount of hydrogen in the specimen varies with these factors [9, 10, 16–18]. Further work is needed to resolve this issue.

Recently Pressouyre and Zmudzinski [13] have suggested that the occurrence of crack nucleation is favoured in the vicinity of the specimen surface during cathodic charging. This implies that the effect of the internal microvoids and/or microcracks induced by hydrogen during hydrogen diffusion in iron gets gradually bigger as the thickness of iron is reduced. Generally the thickness of the iron used in the permeation experiments is thinner than 1 mm. Therefore, it is believed that the input current density should be lower than 1.0 mA cm^{-2} in order to obtain a correct diffusivity of hydrogen in pure iron specimens through electro-permeation experiments in a 10% sulphuric acid solution when adding a recombination poison of about 10 mg As_2O_3 per litre.

6. Conclusions

1. Internal microcracks or microvoids begin to be generated in the vicinity of 1 mA cm^{-2}, and are major trapping sites of hydrogen if hydrogen is charged into iron cathodically. Therefore it is suggested that the input current density must be lower than 1.0 mA cm^{-2} in order to obtain the correct diffusivity of hydrogen

in pure iron throughout an electro-permeation experiment in 10% sulphuric acid solution, adding as a promoter 10 mg l^{-1} As_2O_3.

2. The blisters formed on the surface of an iron specimen during cathodic charging are interconnected to the surface of the specimen through microcracks remaining in the area surrounding the blister.

3. The peak temperature of hydrogen released from an internal microcrack or microvoid is decreased as the hydrogen pressure in it is decreased.

4. The amount of internal microcracks or microvoids and the apparent diffusivity of hydrogen at 458 K are increased and decreased linearly with the square root of applied current density and its reciprocal value, respectively. This implies that the amount of internal microcracks or microvoids increases linearly with that of the hydrogen dissolved into iron during cathodic charging.

References

1. R. A. ORIANI, *Ber. Bunse. Gesellshaft* **76** (1972) 848.
2. T. ADSOKA, Thèse Docteur, Ingénieur, Universite Paris-Sud (1976).
3. I. M. BERNSTEIN and B. B. RATH, *Metall. Trans.* **4** (1973) 1545.
4. I. M. BERNSTEIN, *ibid.* **1** (1970) 3143.
5. *Idem, Mater. Sci. Engng.* **6** (1970) 1.
6. T. TAKEYAMA and H. TAKAHASHI, in Proceedings of JIMS-2 on Hydrogen in Metals (1978) p. 463.
7. H. P. Van LEEUWEN, *Corrosion* **29** (1973) 197.
8. G. M. PRESSOUYRE and I. M. BERNSTEIN, *Acta Metall.* **27** (1979) 89.
9. W. BECK, J. O. M. BOCKRIS, J. McBREEN and L. NANIS, *Proc. R. Soc.* **A290** (1966) 220.
10. S. X. XIE and J. P. HIRTH, *Corrosion* **38** (1982) 486.
11. G. M. PRESSOUYRE, *Acta Metall.* **28** (1980) 895.
12. G. M. PRESSOUYRE and I. M. BERNSTEIN, *Metall. Trans.* **12A** (1981) 835.
13. G. M. PRESSOUYRE and C. ZMUDZINSKI, in Proceedings of 18th Conference on Mechanical Working and Steel Processing, (American Institute of Mining and Metallurgical Engineers, Warrendale, Pennsylvania, 1981).
14. J. Y. LEE and J. L. LEE, *J. Korean Inst. Metals* **21** (1983) 234.
15. *Idem, ibid.* **21** (1983) 427.
16. J. O. M. BOCKRIS and P. K. SUBRAMANYAN, *J. Electrochem. Soc.* **118** (1971) 1114.
17. L. NANIS and T. K. G. NAMBOODHIRI, "Stress Corrosion Cracking and Hydrogen Embrittlement of Iron Based Alloys" (NACE, Houston, Texas, 1977) p. 432.
18. R. POPERLINGS and W. SCHWENK, in Proceedings of 2nd International Congress on Hydrogen in Metals, Paris, Vol. 5A (1977).
19. A. J. KUMNICK and H. H. JOHNSON, *Metall. Trans.* **5** (1974) 1199.
20. W. R. ROBERTSON and A. W. THOMSON, *ibid.* **11** (1980) 553.
21. W. Y. CHOO and J. Y. LEE, *ibid.* **13A** (1982) 135.
22. J. L. LEE and J. Y. LEE, *Metal Sci.* **17** (1983) 426.
23. H. K. LEE and J. Y. LEE, *Acta Metall.* **32** (1984) 131.
24. G. W. HONG and J. Y. LEE, *Scripta Metall.* **17** (1983) 823.
25. J. L. LEE and J. Y. LEE, *Phil. Mag.* in press.
26. J. L. LEE, PhD thesis, Korea Advanced Institute of Science and Technology (1985).
27. G. M. PRESSOUYRE and I. M. BERNSTEIN, *Metall. Trans.* **9A** (1978) 1571.
28. G. M. EVANS and E. C. ROLLASON, *J. Iron Steel Inst.* **207** (1569) 1591.
29. J. L. LEE and J. Y. LEE, *Metall. Trans. B* in press.
30. F. BOZSO, G. ERTL, M. GRUNZE and M. WEISS, *Appl. Surf. Sci.* **1** (1977) 103.
31. K. KUICHI and R. B. McLELLAN, *Acta Metall.* **31** (1983) 961.
32. J. L. LEE and J. Y. LEE, *Scripta Metall.* **19** (1985) 341.
33. A. McNABB and P. K. FOSTER, *Trans. Amer. Inst. Min. Engrs.* **227** (1963) 618.
34. R. A. ORIANI, *Acta Metall.* **18** (1970) 147.

Received 31 October 1986
and accepted 28 January 1987